Evaluation of Internal Heat-Transfer Coefficients for Impingement-Cooled Turbine Airfoils

RAYMOND E. CHUPP* AND HAROLD E. HELMS†
Allison Division of General Motors Corporation, Indianapolis, Ind.

PETER W. MCFADDEN‡
Purdue University, Lafayette, Ind.

AND

TONY R. BROWN§
Midwest Applied Science Corporation, West Lafayette, Ind.

Although internal impingement cooling of the leading edge of gas-turbine airfoils has been shown to be effective, previously available heat-transfer data are not generally applicable to present-day turbine designs because of the unique geometry requirements. An experimental system which allows the ready acquisition of heat-transfer data necessary for thermal design of turbine airfoils is described. A cold-flow model is developed, and the measurement of local heat-transfer coefficients on a full-size model is accomplished by considering Joulean dissipation in very thin platinum strips bonded to the model. Heat-transfer results are given which show the dependence of Nusselt number on Reynolds number, geometry, and chordwise location on the inside leading-edge region of the airfoil. Dimensionless correlations are presented which allow the designer to predict heat transfer for impingement cooling in these geometries for the range of parameters tested.

Nomenclature

A = heat-transfer area for a given strip
d = hole diameter; see Fig. 5
D = leading-edge diameter; see Fig. 4
D_1 = tube width; see Fig. 5
D_2 = tube depth; see Fig. 5
h = heat-transfer coefficient
k = gas thermal conductivity evaluated at the local film temperature
l = distance between the tube and the leading edge; see Fig. 4
Nu = Nusselt number based on hole diameter = hd/k
Pr = Prandtl number of the gas
q = heat-transfer rate by convection from a given strip
Re = Reynolds number for flow through a hole = $4w/\pi d\mu$
s = hole spacing; see Fig. 5
T = temperature
w = gas flow rate per hole
x = chordwise distance along the surface from the stagnation line; see Fig. 4
μ = dynamic viscosity
π = 3.14159...

Subscripts

avg = average for strips located in the leading-edge region where $0 \leq x/D \leq \pi/4$
b = bulk
stag = stagnation strip
w = wall

Presented as Paper 68-564 at the AIAA 4th Propulsion Joint Specialist Conference, Cleveland, Ohio, June 10–14, 1968; submitted June 19, 1968; revision received November 12, 1968.

* Senior Project Engineer, Heat Transfer Section of Engineering Sciences.
† Chief, Engineering Sciences. Member AIAA.
‡ Head, School of Mechanical Engineering; also Consultant to Midwest Applied Science Corporation, West Lafayette, Ind.
§ Heat Transfer Specialist.

I. Introduction

COOLED turbine airfoils have received the attention of gas-turbine designers since World War II when aircraft gas turbines began replacing reciprocating engines. The importance of using cooling air in gas-turbine airfoils to permit higher turbine inlet temperatures is well documented in the open literature. One of the most effective means used to cool the leading edge of a turbine airfoil is to impinge jets of cooling air against its inside surface. This is done by placing a tube inside the hollow airfoil and orienting the tube such that a series of holes machined into the tube are opposite the inside surface of the leading edge. Cooling air introduced into the tube at the base of the airfoil exits through the holes as a series of jets directed at the leading edge. Figure 1 shows a typical impingement-cooled airfoil.

A measure of the effectiveness of a convection-cooling technique such as impingement is given by the internal (airfoil-to-coolant) convective heat-transfer coefficient which gives the heat-transfer rate per unit area per degree temperature difference between the leading edge and the coolant. To design airfoils that use impingement cooling and analyze them,[1] these coefficients must be known as a function of such parameters as the properties of the coolant, coolant flow rate, spatial location, and geometry, i.e., hole diameter, hole spacing, distance between the tube and the leading edge, leading-edge diameter, etc. In a complicated technique such as impingement cooling, these coefficients must be determined experimentally. Unfortunately, most of the data available in the open literature are for relatively large

diameter jets impinging against flat plates.[2–5] These data are not readily applicable to very small diameter jets impinging against a highly curved leading-edge surface of a turbine airfoil. For this reason, an experimental program was undertaken to measure and correlate the heat-transfer coefficients obtainable with jets impinging air into a small radius surface representative of the internal leading-edge region of cooled turbine airfoils.

This paper describes the experimental program conducted to obtain data for impingement cooling and relates some of the results that have been obtained. Some preliminary results of this program were reported previously in a paper reviewing various cooling techniques.[6] The present paper includes a discussion of the basic considerations, a description of the experimental apparatus and procedure, an analysis of the data, a discussion of the results, and the conclusions derived.

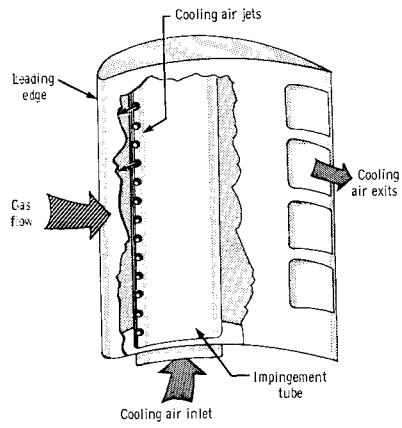

Fig. 1 Schematic of impingement-cooled airfoil.

II. Basic Considerations

Ideally, it would be desirable to measure local heat-transfer coefficients throughout the leading-edge region of a simulated airfoil under a variety of possible geometries and cooling airflows with varying property values approximating engine conditions. This, however, was considered to be impractical from a time, cost, and technical standpoint. Therefore, certain basic considerations were made to simplify the experiments.

One basic consideration was modeling the heat-transfer situation rather than running difficult experiments under actual engine operating conditions. The functional relationship for the local heat-transfer coefficient is

$$h = h \text{ (flow rate, properties, location, geometry)} \quad (1)$$

For constant properties (a good assumption for the engine), Eq. (1) may be written in terms of dimensionless groups as

$$Nu = Nu(Re, Pr, \text{geometry, location}) \quad (2)$$

The functional relationship indicated in Eq. (2) can be found from convenient experiments and then used in design. In particular, cold-flow tests can be run since gas properties are adequately modeled in Nusselt, Reynolds, and Prandtl number. Further, because of the effect of temperature on gas viscosity, mass flow rates in cold flow are smaller than in hot flow for constant Reynolds number. While modeling heat transfer, the Prandtl number was not varied in the testing. However, there is no reason to believe that the accepted $Pr^{1/3}$ could not be used to compensate for Prandtl number other than that used during the experimental program. Also, compressible effects were not important and Mach number was not a variable since it was less than 0.3 in all the tests run.

Another basic consideration was modeling the geometry. In particular, the convenience offered by a larger-than-actual-size airfoil model was investigated. However, because of some recently published impingement heat-transfer results[2] (an independent effect of model size occurs for small values of l/d) and a general concern for modeling the flowfield accurately, it was decided to test actual-size geometries. Only one concession was made; spanwise airfoil twist was not used in the models tested, but rather cylindrical shapes were used. It is felt that this small change in no way compromised the results.

A final basic consideration was made in regard to measuring the local heat-transfer coefficient throughout the leading-edge region. Figure 2 shows several positions along the leading-edge surface inside a typical cooled airfoil. Position A is at the stagnation point ahead of the jet stream. Position B is midway between jets. Position C is the stagnation point ahead of a second jet stream. Because of spanwise variations in local flow due to the jets, the heat-transfer coefficient will vary considerably from positions A to C depending on the hole and leading-edge geometries and the flow through the holes. In addition, the value of h will vary chordwise around the leading edge, e.g., from position C, because of changing airflow velocities and patterns away from the stagnation point. This chordwise variation of h will be a strong function of the flow split as the flow separates and goes to either side of the tube. It would be desirable to obtain point-by-point evaluation of the heat-transfer coefficient, but this was determined to be impractical. Therefore, a value of h averaged in the spanwise direction was measured and evaluated at as many chordwise positions as possible in and near the leading edge. This was found to be a feasible and practical approach.

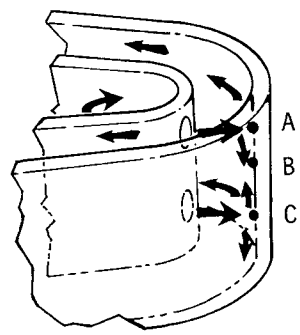

Fig. 2 Schematic of impingement-cooled airfoil leading edge.

III. Experimental Apparatus and Procedure

In the experiments, an actual-size plastic model of the inside leading-edge region of a turbine airfoil was used. A movable supply tube provided the impingement air via jet arrays. Heat transfer from the inside leading-edge region was obtained by Joulean heat dissipation in nine thin, parallel platinum strips epoxy cemented spanwise on the surface. The strips were 0.0002 in. thick, 0.020 in. wide, and 0.875 in. long; the strips were spaced 0.001 in. apart. The thickness of the epoxy layer on the plastic was about 0.001 in. On installation, the platinum strips were pressed into the epoxy; care was taken not to get any cement on the exposed surface of the platinum and, at the same time, to make the resulting surface (alternating platinum and epoxy) as smooth as possible. The thickness of any resulting surface roughness elements was considerably less than the thickness of the epoxy layer.

One of the platinum strips was centered on the surface of the inside leading edge and served as the stagnation strip.

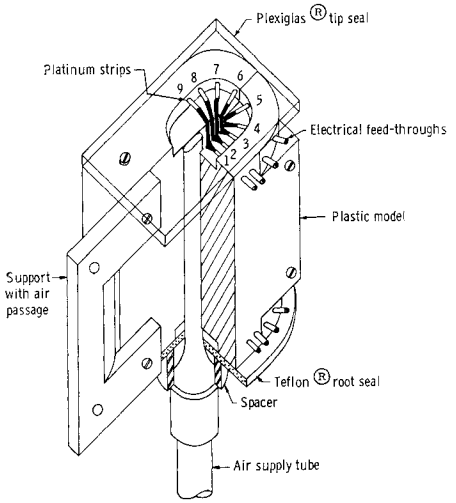

Fig. 3 Schematic of experimental model.

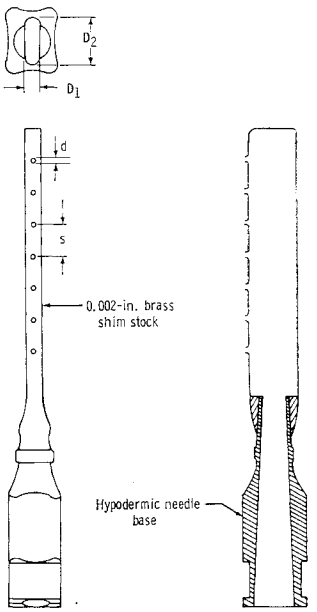

Fig. 5 Schematic of typical impingement tube.

The remaining strips were located on either side of the stagnation strip, thus providing chordwise varying heat transfer.

A schematic drawing of the experimental test model is shown in Fig. 3 (the platinum strips are exaggerated for clarity). The actual locations of these strips were concentrated in the leading-edge radius region as is shown in Fig. 4. The plastic model was sealed at the tip with a Plexiglas® seal (for visual inspection during testing) and at the root with a Teflon® seal. The Teflon® seal was a sliding seal to allow freedom of adjustment of the impingement tube. The impingement air was exhausted chordwise.

Several impingement tubes were tested. These tubes had a single row of circular holes as shown schematically in Fig. 5. The instrumented model and impingement (air supply) tube were installed in a pressure vessel for the tests, as shown in Fig. 6. Testing was done at convenient pressure levels (modeling engine operating conditions when necessary) without requiring the plastic model assembly to withstand large pressure differences. A positioning mechanism with sliding seals was installed on the bottom of the pressure vessel.

The wall-temperature distribution was obtained from a calibration of electrical resistance vs temperature for each of the platinum strips using the measured electrical resistance for each strip. All electrical measurements were taken using a digital data acquisition system; these measurements were permanently recorded on punched tape to facilitate subsequent computer analysis.

Cooling air was supplied to tubes from cylinders of compressed air. A regulator valve on the cylinders was used to reduce the pressure to desired test levels. The flow rate was controlled by a flow control valve located downstream of the test section. The airflow rate was measured with a rotameter (accurate within 1% of full scale) for high flow rates and a wet test meter (accurate within $\frac{1}{2}$%) for low flow rates. The inlet air pressure was measured with a 0–300-psi pressure gage (accurate within $\frac{1}{2}$% of full scale).

During the experiments, 14 tubes and 2 different plastic leading-edge models were tested. The hole geometries varied from one tube to the next so that a range of hole diameters from 0.006 to 0.26 in. and hole spacings from 0.0312 to 0.125 in. was tested. The leading-edge diameters of the two models tested were 0.094 and 0.040 in.; most of the data were taken using the model having the 0.094-in.

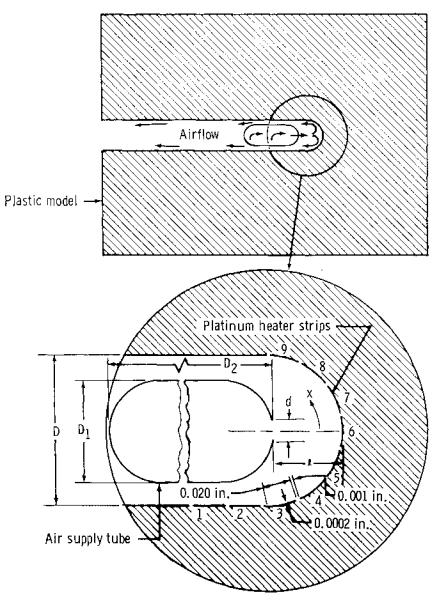

Fig. 4 Detailed view of experimental model.

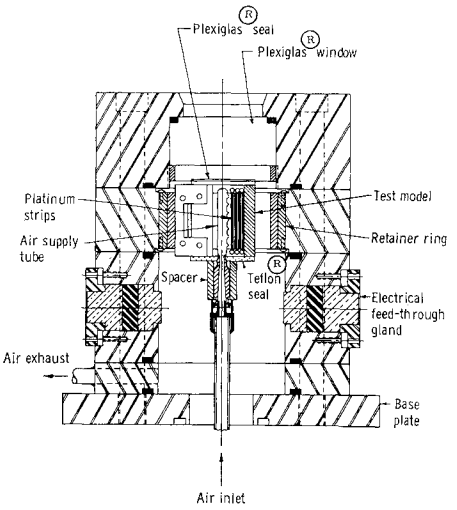

Fig. 6 Schematic of top half of pressure vessel.

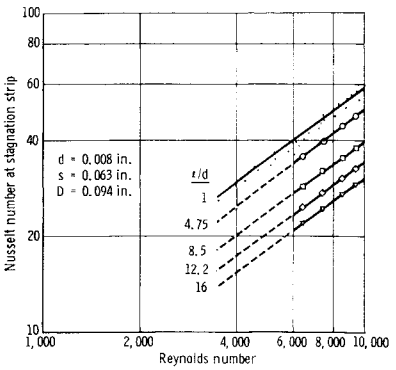

Fig. 7 Nusselt number at stagnation strip vs Reynolds number for a typical impingement tube tested.

diam. For each tube and leading-edge model combination, the total airflow rate through the tube was varied from 9 to 50 standard cubic feet per hour and the distance between the tube and leading edge l varied from 0.006 to 0.160 in. with the tube centered in the leading-edge region. Since the tube was centered, a near-equal flow split of air around the tube was obtained. In the first part of the testing, the inlet pressure was varied from 50 to 250 psig. In later tests, however, only one or two inlet pressures were used after it was determined that the effect of pressure for these incompressible flow tests could be accounted for by correlating the data in terms of Reynolds number.

IV. Data Analysis

From the raw test data, the local convective heat-transfer coefficient for each strip was calculated using its definition

$$h = q/A(T_w - T_b) \tag{3}$$

The bulk temperature T_b was calculated using the measured impingement air supply temperature and a heat balance. The wall temperature T_w used was the strip temperature obtained from the measured resistance of the strip. This temperature was a spanwise average temperature for the strip; thus, the value of h calculated using Eq. (3) was also spanwise averaged. An analysis was performed to show that, even though the periodic spanwise temperature variation is complex, the measured resistance (except for a small end correction which was neglected) gives the true average temperature since the electrical resistance varies linearly with temperature. The area A in Eq. (3) was taken to be 1.05 times the exposed strip area to compensate conservatively for heat transfer to the air from the epoxy between the strips.

The Joulean heat dissipation in each strip was not equal to the convective heat-transfer rate from the strip to the cooling air. Because of heat losses through the plastic and heat exchange with other strips at different temperatures, a conduction correction was applied to each strip. This correction was determined using a standard finite-difference conduction program and was equal to, at most, 15% of the dissipation.

From the h computed using Eq. (3) and the other measured parameters, the Nusselt number for each strip based on the hole diameter and the Reynolds number for flow through the holes could be determined.

Error Analysis

An estimation of the various errors in the experiments was made to determine the accuracy of the data obtained. The heat-transfer rate was considered to be accurate to within 4%. Average wall temperatures were determined to be within 1°F; at the stagnation strip, the bulk temperature was measured within 1°F, giving an accuracy in $T_w - T_b$ of within 2°F out of about 60°F. The heat-transfer area was determined to within 1%. Hence, convection coefficients were determined to within 8% maximum. The maximum flow-rate error occurred at the changeover from the rotameter to the wet test meter (at about $\frac{1}{3}$ full scale of the rotameter), yielding a possible 3% error.

It would be desirable to check experimentally the conduction correction and the heat balance made in reducing the data. In future tests, attempts will be made to make these experimental checks.

V. Discussion of Results

The independent parameters of primary interest in the present experimental program were the Reynolds number, hole diameter, hole spacing, distance from the tube to the leading edge, leading-edge diameter, and the chordwise

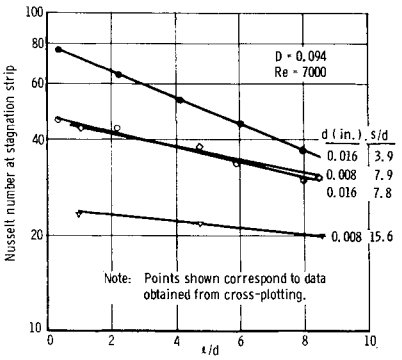

Fig. 8 Nusselt number at stagnation strip vs l/d for typical hole geometries.

location. These parameters were varied systematically to obtain the results given herein. It was found that, when geometry and location were held fixed and only Reynolds number was varied, Nusselt number varied with Reynolds number to a power, as was expected. This result simplified correlation of the data, as will be seen in the following paragraphs.

Consider the heat transfer near the stagnation line. Figure 7 shows the experimentally determined relationships between the Nusselt number for the stagnation strip, Nu_{stag}, and the parameters Re and l/d for a typical impingement tube tested. As indicated, the slope of Nu_{stag} vs Re is nearly the same for all l/d values tested. This indicates that the effect of l/d on Nu_{stag} can be considered separately from the effect of Re. To see the influence of l/d, a plot of Nu_{stag} vs l/d for typical hole geometries and a given Reynolds number is shown in Fig. 8. Figure 8 was obtained by cross-plotting curves, such as those in Fig. 7, at a given value of Re. Figure 8 indicates that Nu_{stag} varies nearly exponentially with l/d, and the slope and intercept of this variation are functions of the hole geometry. In addition, Nu_{stag} vs l/d is a function of the leading-edge diameter (D).

The data for Nu_{stag} were empirically correlated with the other parameters using plots such as those in Figs. 7 and 8 to indicate the form of the functional relationships. To obtain correlations which are dimensionless, the hole diameter was picked as the characteristic dimension. Neglecting the effect of Pr,

$$Nu_{stag} = Nu_{stag}(Re, l/d, s/d, D/d) \tag{4}$$

Empirical correlations were then obtained by fitting the data to various equations derived from plots of the data using the parameters given in Eq. (4) as the independent variables. The equation which best fits the data for $3000 \leq Re \leq 15{,}000$, $4 \leq s/d \leq 16$, $1 \leq l/d \leq 10$, and $1.5 \leq D/d \leq 16$ is

$$Nu_{stag} = 0.44\, Re^{0.7}(d/s)^{0.8} \times \exp[-0.85(l/d)(d/s)(d/D)^{0.4}] \tag{5}$$

Equation (5) fits the data with an average absolute deviation of 9%. This equation then fits the data well since the deviation is of the order of estimated error in the data. The terms in front of the exponential in Eq. (5) account for the intercept variations in Fig. 8; the last two terms in the exponential account for the slope variations. The d/D term did not seem to affect the intercept for the data taken. Equation (5) could be simplified by combining the first two terms in the exponential, yielding an (l/s) term. This simplification, however, would conceal the fact that d was used as the characteristic dimension.

Equation (5) was obtained by best fitting the data using an optimization routine. This equation could not be fitted using a standard least-squares technique since the powers on (l/d), (d/s), and (d/D) in the exponential term could not be obtained even after taking the logarithms of both sides of the equation and fitting the result. The most expeditious method found for fitting this type of equation to the data was to use a computer optimization program which randomly perturbed each of the unknown constants until the best fit of the equation to the data was obtained.

Another independent parameter considered was the chordwise distance x from the stagnation line. Figure 9 shows a plot of normalized Nusselt number $Nu(x)/Nu(x = 0)$ vs x/d with l/d as a parameter and Re a constant for a typical impingement tube. The values of x used in Fig. 9 correspond to the distances from the stagnation line to the middle of the strips except for the stagnation strip. The x value employed for the stagnation strip was $\frac{1}{4}$ of the strip width, i.e., the average distance away from the actual stagnation line for this strip. The Nusselt number at the stagnation line, which was used to calculate $Nu(x)/Nu(x = 0)$, was determined by extrapolating the data back to $x = 0$. Figure 9 shows that $Nu(x)/Nu(x = 0)$ depends primarily on x/d and to a lesser extent on l/d. It was also found that this normalized Nusselt number is only a weak function of s/d (at least for $l/d \gg 1$) and is independent of Re within the accuracy of the data.

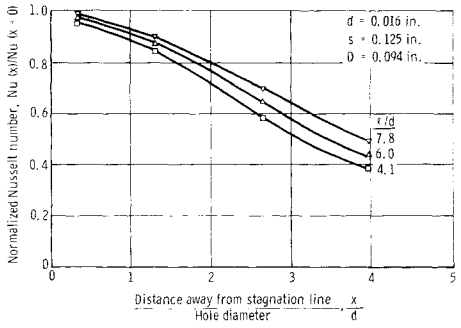

Fig. 9 Normalized Nusselt number vs distance away from stagnation line for a typical impingement tube tested.

The over-all effect of the parameter x can be found by evaluating an average Nusselt number Nu_{avg} for impingement. In this investigation, Nu_{avg} was an arithmetic average of the Nusselt number for strips located in the leading edge region such that $0 \leq x/D \leq \pi/4$.

Figure 10 shows the variation of Nu_{avg} with Re and l/d for the same impingement tube considered in Fig. 7. Comparing Figs. 7 and 10 indicates that Nu_{stag} and Nu_{avg} vary similarly with Re and l/d for a given hole geometry except Nu_{avg} varies less with l/d than does Nu_{stag}. Correlation of Nu_{avg} with the parameters given in Eq. (4) was obtained using methods similar to those used for Nu_{stag}. The equation which best fits the data for the same range of parameters as given for Eq. (5) is

$$Nu_{avg} = 0.63\, Re^{0.7}(d/s)^{0.5}(d/D)^{0.6} \times \exp[-1.27(l/d)(d/s)^{0.5}(d/D)^{1.2}] \quad (6)$$

Equation (6) fits the data with an average absolute deviation of 8.7% and thus, this equation fits the data well. Equation (6) indicates that the term d/D affects the intercept of Nu_{avg} vs l/d as well as the slope. It should be stressed that Eqs. (5) and (6) should only be used within the limits of the data taken, and extrapolation outside these limits could lead to erroneous results.

In addition to the variables mentioned in the preceding paragraphs, the Nusselt number is also a function of the chordwise thermal boundary condition. During testing, data were taken for the wall boundary condition varying from isothermal to constant heat flux. Results for both extremes were identical for the stagnation strip within experimental error, as expected. Also, as expected, the thermal boundary condition had only a modest effect on the Nusselt number away from the stagnation strip, with differences being 15% at most.

Comparison with Other Investigators

The results obtained in this program agree qualitatively with results previously published in the open literature.[2-5] A major difference, however, is in the variation of Nu_{stag} with l/d for small values of l/d. Figure 8 shows that, in this investigation, Nu_{stag} increases as l/d decreases to unity. Results from other investigations[2,5] for single jets indicate that the Nusselt number 1) increases as l/d decreases to 8 or 10 and 2) decreases as l/d decreases further. The difference between these two results could be due to the spanwise averaging of the Nu_{stag} that has occurred in this investigation. This difference could also be due to a difference in the turbulence creased by the jets in the two cases. In the present experiments, the jets were sharp-edged orifices which would promote turbulence regardless of the l/d value; in the previous work, the jets were smooth nozzles and the turbulence of the impinging air was a function of l/d since the turbulence was due primarily to an interaction of the jet with the surrounding air. If this is the case, then the variation of Nusselt number with l/d would be different for the two experiments for $l/d < 10$.

VI. Conclusions

The results reported herein show that the experimental system described can provide basic heat-transfer data for impingement cooling of the leading edge of turbine airfoils within the basic considerations given. The dimensionless correlations of the data presented can be readily applied to design and analysis of turbine airfoils. The present experimental work is being continued using an extended range of parameters and different hole configurations. In addition,

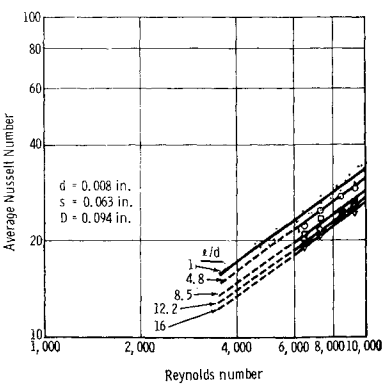

Fig. 10 Average Nusselt number vs Reynolds number for a typical impingement tube tested.

compressible effects and different flow distributions around the tube are being investigated. The results of this additional work will be published in a future paper.

References

[1] Matchett, J. D., Colborn, J. N., and Ahles, A. F., "A Comparison of Calculated and Measured Temperature Distributions in Forced-Convection Air-Cooled Gas Turbine Airfoils," Paper 67-WA/GT-4, 1967, American Society of Mechanical Engineers.

[2] Gardon, R. and Cobonpue, J., "Heat Transfer Between a Flat Plate and Jets of Air Impinging on It," *International Developments in Heat Transfer, Proceedings, 2nd International Heat Transfer Conference*, American Society of Mechanical Engineers, 1962, pp. 454–460.

[3] Huang, G. C., "Investigations of Heat Transfer Coefficients for Air Flow Through Round Jets Impinging Normal to a Heat-Transfer Surface," *Journal of Heat Transfer, Transactions of the American Society of Mechanical Engineers*, Vol. 85C, 1963, pp. 237–245.

[4] Gardon, R. and Akfirat, J. C., "Heat Transfer Characteristics of Impinging Two-Dimensional Air Jets," *Journal of Heat Transfer, Transactions of the American Society of Mechanical Engineers*, Vol. 88C, 1966, pp. 101–108.

[5] Gardon, R. and Akirfat, J. C., "The Role of Turbulence in Determining the Heat-Transfer Characteristics of Impinging Jets," *International Journal of Heat and Mass Transfer*, Vol. 8, 1965, pp. 1261–1272.

[6] Helms, H. E. and Emmerson, C. W., "Analysis and Testing of Air-Cooled Turbine Rotor and Stator Blades," Paper 65-WA/GTP-10, 1965, American Society of Mechanical Engineers